Self-Assembly

DOI: 10.1002/anie.201201816

Thermoresponsive Assembly of Charged Gold Nanoparticles and Their Reversible Tuning of Plasmon Coupling**

*Yiding Liu, Xiaogang Han, Le He, and Yadong Yin**

Plasmonic metal nanostructures have been intensively studied for a wide range of applications such as chemical sensing, optoelectronics, and photothermal therapy, because of their unique optical properties caused by localized surface plasmon resonance (LSPR).[1] Since the assembly of plasmonic nanoparticles into secondary structures may induce near field coupling of surface plasmons between adjacent particles, new optical properties can be obtained, inducing shifts of plasmonic peaks, and the generation of "hot spots" that are very useful for enhancing Raman scattering.[2] Of particular interest is the reversible assembly of such plasmonic nanostructures, which is expected to enable dynamic tuning of the surface plasmon coupling in response to the external stimuli, and therefore produce active optical materials for applications such as color signage, bio- and chemical detection, and environmental sensing.[3] However, despite extensive studies on nanoparticle assembly,[2a,4] it remains a great challenge to develop stimuli-responsive systems with reversibly tunable plasmonic properties. In the few available reports for gold nanoparticles (AuNPs), some are designed to respond to pH changes,[2c,5] while others involve thermoresponsive polymers so that the systems are sensitive to temperature variations.[6]

Recently, it was found that charged AuNPs can self-assemble into linear structures in aqueous media and show significantly altered optical properties because of surface plasmon coupling.[2a,7] The linear assembly is believed to be the result of a balance between various interparticle attractive and repulsive forces, such as van der Waals attraction and electrostatic repulsion, and is primarily promoted by the relatively weak electrostatic repulsion experienced by a AuNP during end-on attachment to an existing nanochain relative to side attachment. We also reported recently that when the AuNPs are capped with sufficiently strong ligands, such as bis(*p*-sulfonatophenyl)-phenylphosphine (BSPP), the assembly process becomes reversible, with the linear chain structures forming at high ionic strength, and dissociating after dilution.[8] It is believed that the short-range steric repulsion enabled by the BSPP layer counters the van der Waals attraction when the particles are brought into close contact, and thus enables the reversible assembly and disassembly.

While the van der Waals attraction mainly depends on the properties of the nanoparticles themselves, such as density, shape, and volume, the electrostatic interaction depends not only on the surface properties of the nanoparticles but also the properties of their surroundings, such as the dielectric constant of the solvent, the ionic strength, pH, and temperature.[4f,7a,9] Herein, we demonstrate the thermoresponsive assembly and disassembly of charged AuNPs through the manipulation of the electrostatic interactions by temperature variation, and further show dynamic and reversible tuning of the surface plasmon coupling by controlling the temperature of the solution. Based on experimental measurements and theoretical calculation, we reveal that the reversible assembly and disassembly can be attributed to the temperature dependence of the surface charges on the colloidal nanoparticles.

Negatively charged AuNPs covered with BSPP ligands were synthesized by using the classic citrate reduction method followed by a ligand exchange process. Then the AuNPs, about 15 nm in diameter, were dispersed in an aqueous mixture of 0.09 M NaCl and 2 wt % agarose at 70 °C. Cooling the sample down greatly increased the viscosity of the system and eventually converted the solution into a hydrogel when the temperature is below 40 °C. By sweeping the temperature in the range of 40–5 °C, AuNPs can be assembled or disassembled, and show temperature-dependent optical properties (Figure 1 a). The sample at high temperature appeared ruby red, indicating a disassembled state, while at low temperature it became dark blue, suggesting a linear chain structure as described in earlier reports.[7,8] As shown in the temperature-dependent extinction spectra in Figure 1 b,c, when the temperature was lowered from 40 °C, the plasmonic peak originally at about 525 nm gradually decreased in intensity, while a shoulder at longer wavelengths started to develop and eventually evolve into a distinct peak at about 685 nm upon the temperature reaching 5 °C. This new peak represents a 1D longitudinal plasmon coupling between AuNPs, revealing the chain structure of the assemblies.[2a,8,10] The red-shift of the original 525 nm peak to about 560 nm is most likely because of the irregularity of the chain-like aggregates which results from the high salt concentration in our systems.[11] When the same sample was heated from 5 °C back to 40 °C, the extinction spectra gradually reverse

[*] X. Han, L. He, Prof. Y. Yin
Department of Chemistry, University of California
Riverside, CA 92521 (USA)
E-mail: yadong.yin@ucr.edu
Homepage: http://faculty.ucr.edu/~yadongy/
Y. Liu, Prof. Y. Yin
Materials Science and Engineering Program
University of California, Riverside, CA 92521 (USA)

[**] Y.Y. thanks the US Army Research Office (grant number W911NF-10-1-0484), 3M for a Nontenured Faculty Grant, and DuPont for a Young Prof. Grant. Y.Y. is a Cottrell Scholar of the Research Corporation for Science Advancement. The use of the Central Facility for Advanced Microscopy and Microanalysis at UCR is also acknowledged.

Supporting information for this article is available on the WWW under http://dx.doi.org/10.1002/anie.201201816.

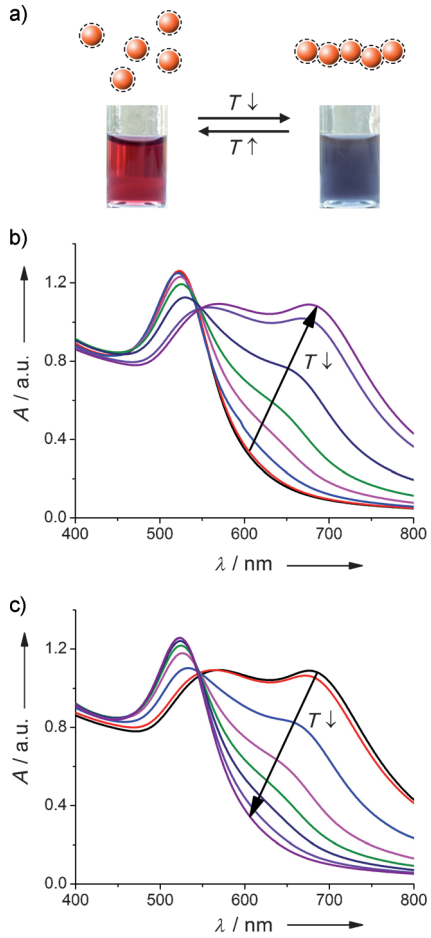

Figure 1. The thermoresponsive tuning of plasmonic properties of charged colloidal AuNPs: a) AuNPs switching between the disassembled and assembled states in response to temperature changes, b) the extinction spectra of a typical AuNP dispersion when cooled from 40 °C to 5 °C, and c) the extinction spectra of the same sample when heated from 5 °C back to 40 °C. There is a 5 °C temperature difference between each neighboring spectrum.

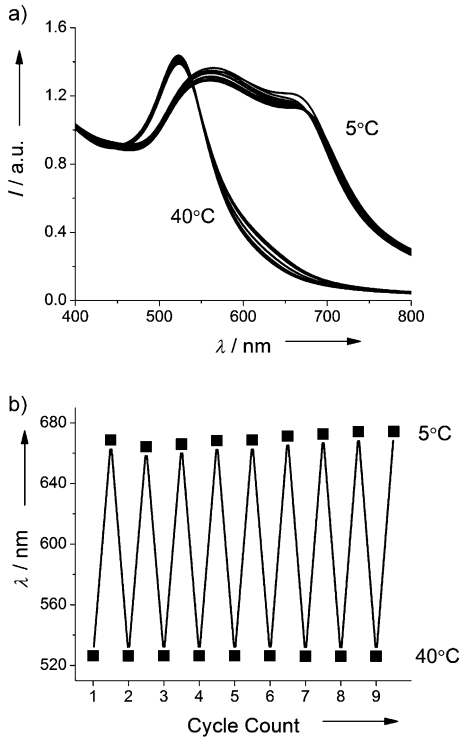

Figure 2. a) The extinction spectra of a typical AuNP dispersion during nine cycles of repeated heating (at 40 °C) and cooling (at 5 °C). b) The repeated switching of plasmonic peak positions (ISP peak at 40 °C and CSP peak at 5 °C) for nine cycles.

direction and fully recover the single isotropic surface plasmon (ISP) band, suggesting the disassembly of the chains into isolated nanoparticles. The assembly and disassembly processes also occur in the AuNP solution containing no agarose. The presence of the agarose hydrogel network, however, helps to limit extensive chain growth, prevent precipitation of the assemblies, and ensure uniform distribution of the AuNPs in the sample, so that a consistent optical tuning can be achieved and recorded.[12]

To investigate the stability and reversibility of the system, a similar sample was prepared and cycled 9 times between 5 °C and 40 °C. As shown in Figure 2a, the recorded spectra essentially show two bands of nearly overlapped curves corresponding to extinction profiles at high and low temperatures, respectively. Figure 2b plots the peak positions of the coupled surface plasmon (CSP) band at 5 °C and the ISP band at 40 °C, further demonstrating the complete reversibility of the thermoresponsive optical switching. Compared to the pH-responsive assembly systems, our system exhibits impressive reversibility and reproducibility.[5a,c]

Combining the two major interactions commonly considered in the Derjaguin–Landau–Verwey–Overbeek (DLVO) theory results in a net potential that is predicted to approach a value of negative infinity upon particle contact.[9,13] Apparently, such an infinitely deep primary minimum is not consistent with the reversible assembly observed in this study.[14] Therefore, non-DLVO interactions accounting for short-range repulsion cannot be neglected when nanoparticles begin to contact.[15] Theoretically, whether nanoparticles are in assembled or disassembled states as well as the reversibility of nanoparticle assemblies should be determinable by examining the interparticle energy diagrams under specific conditions. If the interparticle energy minimum appears at a short interparticle distance, the assembled state is thermodynamically preferable; otherwise, the disassembled state is preferred.[9,16] The total interaction energy (V_{TOT}) between colloidal nanoparticles is the sum of electrostatic energy (V_{elec}), van der Waals potential energy (V_{vdW}) and short-range repulsion energy (V_{SR}) [Eq. (1)].[7a,9,13] For nano-

$$V_{TOT} = V_{elec} + V_{vdW} + V_{SR} \quad (1)$$

scale spherical particles, the electrostatic and van der Waals potential energy can be expressed by Equations (2) and (3).[7a]

$$V_{elec} = 2\pi\varepsilon_s\varepsilon_0 a\psi_0^2(T)\ln\{1+\exp[-a\kappa(R-2)]\} \quad (2)$$

$$V_{vdW} = -\frac{A}{6}\left(\frac{2}{R^2-4}+\frac{2}{R^2}+\ln\frac{R^2-4}{R^2}\right) \quad (3)$$

In Equation (2), $\varepsilon_s\varepsilon_0$ is the dielectric constant of the solvent, a is the radius of the particle, ψ_0 is the surface potential of the particle, T is absolute temperature, κ^{-1} is the Debye length [shown in Eq. (4)], and $R = r/a$ where r is the distance

$$\kappa^{-1} = \frac{\varepsilon_s\varepsilon_0 k_B T}{2000 e^2 N_A I} \tag{4}$$

between the neighboring particle centers. In Equation (3), A is the Hamaker constant between particles in the solvent which is 3×10^{-19} J for Au-H_2O-Au.[17] In Equation (4), k_B is the Boltzmann constant, e is the charge of electron, and I is the ionic strength of the solvent. In this system, the short-range repulsion is mainly due to the steric interactions between BSPP and the hydration force experienced by the interacting AuNPs. Without referring to the precise details of the short-range forces, we find it convenient to resort to the mean Born potential formulation developed previously for the examination of reversible coagulation or adsorption phenomena,[13] as shown in Equation (5), in which σ_c is the collision diameter with a typical value of 0.5 nm.[13,15b]

$$V_{SR} = 4A\left(\frac{\sigma_c}{a}\right)^6\left(\frac{4!}{10!}\right)\frac{1}{R}\left(\frac{R^2-14R+54}{(R-2)^7}+\frac{-2R^2+60}{R^7}+\frac{R^2+14R+54}{(R+2)^7}\right) \tag{5}$$

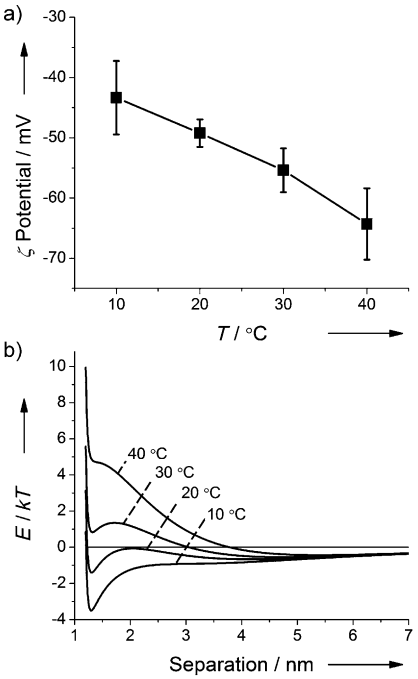

Figure 3. a) Zeta potential versus temperature plotted for colloidal AuNPs in 0.09 M NaCl aqueous solution. b) Interparticle energy versus interparticle distance plot of AuNPs in 0.09 M NaCl aqueous solution.

According to Equation (2), electrostatic interaction is mainly affected by temperature, Debye length, dielectric constant of the solvent, and particle surface potential. The first three parameters can be directly obtained or derived, while the particle surface potential in solutions with defined ionic strength and temperatures can be measured. Figure 3a shows the zeta potential values for AuNPs dispersed in a 0.09 M NaCl solution at four different temperatures, which was found to change from −64.3 mV to −43.3 mV with the decrease in temperature from 40 °C to 10 °C. The nearly linear increase in the magnitude of zeta potential with temperature is consistent with the results reported in the literature, and it is often attributed to the changes in surface adsorption/desorption equilibrium, charge dissociation equilibrium, and the diffuse double-layer thickness.[18] Our calculation shows that the change in zeta potential with temperature leads to a prominent change of electrostatic energy. With an assumed ligand layer thickness of 0.5 nm (Supporting Information), Figure 3b plots the total interaction energy versus interparticle distance, as calculated according to Equations (1)–(5). The energy diagrams show obvious differences for cases at different temperatures. The primary energy maximum, which plays a role as an energy barrier for the assembly process, gradually vanishes with decreasing temperature. At the same time, an energy well at about 1.3 nm gradually evolves, which is in favor of a stable assembled state. This result is in agreement with experimental observations that a disassembled or isolated state is energetically favored for AuNPs at higher temperatures such as 40 °C; while at low temperatures such as 10 °C or lower, AuNPs can stay in the assembled state because of the presence of a well-defined energy well. Meanwhile, the considerably shallow energy well at low temperatures (< 4 kT) is critical for the reversible assembly–disassembly processes.[19]

The ionic strength of the solution has a profound effect on electrostatic interactions. As expected, the salt concentration plays an important role in governing the particle interaction energy and therefore the assembly behavior. Figure 4 compares the extinction spectra of the samples with lower (0.05 M) and higher (0.13 M) NaCl concentrations relative to the typical value (0.09 M) that we tested. At a low salt concentration, no extensive assembly of AuNPs occurred, resulting in a CSP band that appeared only as a shoulder even at 5 °C. At a high salt concentration, assembly of AuNPs was difficult to prevent, with a CSP band prominent even at high temperatures such as 40 °C. Calculation of the particle interaction energy for the case of low salt concentrations by using the measured zeta potential values suggests that even though distinct energy wells form throughout the entire temperature range, the overall positive interaction energy and the high primary energy maximum make it difficult to form assemblies (Figure 4c). In the case of high salt concentrations, a small interparticle distance is energetically preferable, as suggested by the considerably deep energy wells in the calculated particle interaction energy diagram in Figure 4d, suggesting a significantly higher tendency to assemble.

The concentrations of both nanoparticles and agarose have been found to affect the extent of the AuNP assembly and consequently the plasmonic properties. When other parameters are fixed, the variation in the concentration of AuNPs change the average size of the assemblies, as expected from the mass action kinetic analysis.[20] When assembled at 5 °C, the CSP peak shifts more to the red and shows a continuously increasing intensity at higher AuNP concen-

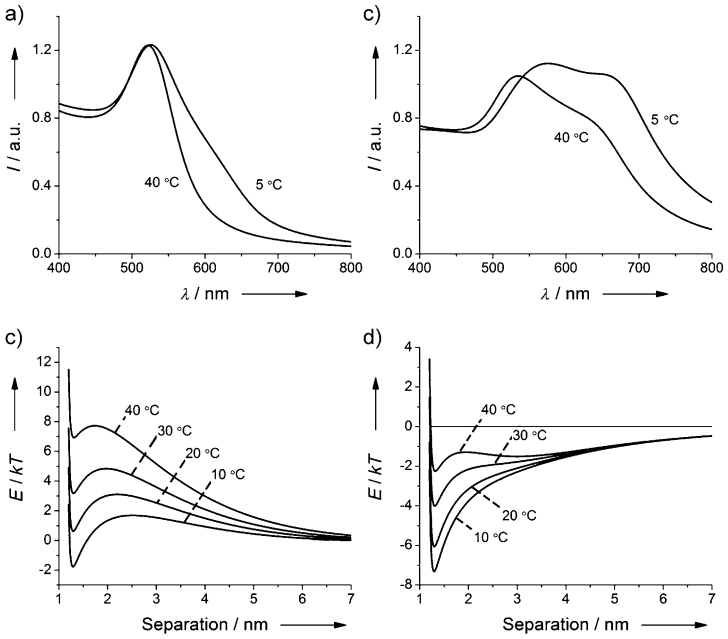

Figure 4. The extinction spectra measured at 40 and 5 °C for AuNP dispersions containing a) 0.05 M and b) 0.13 M NaCl solutions, and the plots showing the interparticle energy versus separation calculated for various temperatures for AuNP dispersions containing c) 0.05 M and d) 0.13 M NaCl solutions.

trations. The concentration of agarose does not significantly affect the optical property of the AuNPs in the disassembled form at high temperatures, however, it changes the average chain length during the assembly of the AuNPs because the gel density determines the local availability of the AuNPs.[12b] As a result, the CSP peak shifts to longer wavelengths when the particles are assembled at 5 °C in a diluted agarose solution. Because a higher agarose concentration is beneficial to maintaining the stability of AuNP assemblies against precipitation, we found 2 wt% to be a good compromise between the plasmon shift and the stability against precipitation.

In summary, we have studied the thermoresponsive assembly and disassembly of colloidal AuNPs in aqueous solution and demonstrated the reversible tuning of plasmon coupling by controlling the temperature of the colloidal dispersion. The thermoresponsive tuning was made possible by the temperature dependence in the zeta potential of the charged nanoparticles which allows reversible manipulation of the electrostatic interactions by temperature variation. The dynamic tuning of the surface plasmon coupling demonstrated in this work represents an important step towards the development of novel LSPR-based functional optical devices.

Experimental Section

Negatively charged AuNPs were synthesized by the classic citrate reduction method followed by a ligand exchange process. Typically, $HAuCl_4 \cdot 3H_2O$ (19 μL, 1 g mL^{-1}) aqueous solution was added to boiling deionized (DI) water (95 mL) under stirring, followed by the addition of an aqueous solution of tri-sodium citrate (5 mL, 1 wt%). After boiling for 20 min, the solution gradually turned from colorless to dark red. Upon cooling down to room temperature, the solution was mixed with an aqueous solution of BSPP (0.5 mL, 40 mg mL^{-1}) and then stirred for 12 h. The AuNPs were isolated by centrifugation, washed with DI water (18 MΩ cm) 2 times, and dispersed in 10 mL of water. To prepare the AuNP/gel sample, a solution containing modified AuNPs (100 μL) was mixed sequentially with a BSPP solution (50 μL, 40 mg mL^{-1}), an agarose sol (1 mL, 2 wt%) preheated at about 70 °C, and a NaCl solution (100 μL) of various concentrations. The mixture was transferred to a plastic cuvette after ensuring homogeneity. For both optical and zeta potential analyses, the samples were stabilized at defined temperatures (variation < 0.2 °C) for 10 min before each measurement.

Received: March 6, 2012
Revised: May 3, 2012
Published online: May 23, 2012

Keywords: colloidal interactions · nanoparticles · plasmon coupling · reversibility · self-assembly

[1] a) J. N. Anker, W. P. Hall, O. Lyandres, N. C. Shah, J. Zhao, R. P. Van Duyne, *Nat. Mater.* **2008**, *7*, 442–453; b) M.-S. Hu, H.-L. Chen, C.-H. Shen, L.-S. Hong, B.-R. Huang, K.-H. Chen, L.-C. Chen, *Nat. Mater.* **2006**, *5*, 102–106; c) X. Huang, P. Jain, I. El-Sayed, M. El-Sayed, *Lasers Med. Sci.* **2008**, *23*, 217–228.

[2] a) S. Lin, M. Li, E. Dujardin, C. Girard, S. Mann, *Adv. Mater.* **2005**, *17*, 2553–2559; b) S. Nie, S. R. Emory, *Science* **1997**, *275*, 1102–1106; c) P. Taladriz-Blanco, N. J. Buurma, L. Rodriguez-Lorenzo, J. Perez-Juste, L. M. Liz-Marzan, P. Herves, *J. Mater. Chem.* **2011**, *21*, 16880–16887.

[3] a) M.-Q. Zhu, L.-Q. Wang, G. J. Exarhos, A. D. Q. Li, *J. Am. Chem. Soc.* **2004**, *126*, 2656–2657; b) R. Klajn, K. J. M. Bishop, B. A. Grzybowski, *Proc. Natl. Acad. Sci. USA* **2007**, *104*, 10305–10309; c) D. Li, Q. He, Y. Cui, J. Li, *Chem. Mater.* **2007**, *19*, 412–417; d) R. Elghanian, J. J. Storhoff, R. C. Mucic, R. L. Letsinger, C. A. Mirkin, *Science* **1997**, *277*, 1078–1081; e) T. S. Sreeprasad, T. Pradeep, *Langmuir* **2011**, *27*, 3381–3390.

[4] a) M. M. Maye, I. I. S. Lim, J. Luo, Z. Rab, D. Rabinovich, T. Liu, C.-J. Zhong, *J. Am. Chem. Soc.* **2005**, *127*, 1519–1529; b) Z. Lu, J. Goebl, J. Ge, Y. Yin, *J. Mater. Chem.* **2009**, *19*, 4597–4602; c) Y. Min, M. Akbulut, K. Kristiansen, Y. Golan, J. Israelachvili, *Nat. Mater.* **2008**, *7*, 527–538; d) T. Kim, K. Lee, M.-s. Gong, S.-W. Joo, *Langmuir* **2005**, *21*, 9524–9528; e) S. Corezzi, C. De Michele, E. Zaccarelli, P. Tartaglia, F. Sciortino, *J. Phys. Chem. B* **2009**, *113*, 1233–1236; f) Y. Wang, G. Chen, M. Yang, G. Silber, S. Xing, L. H. Tan, F. Wang, Y. Feng, X. Liu, S. Li, H. Chen, *Nat. Commun.* **2010**, *1*, 87.

[5] a) Z. Sun, W. Ni, Z. Yang, X. Kou, L. Li, J. Wang, *Small* **2008**, *4*, 1287–1292; b) P. Hazarika, B. Ceyhan, C. M. Niemeyer, *Angew. Chem.* **2004**, *116*, 6631–6633; c) S. Z. Nergiz, S. Singamaneni, *ACS Appl. Mater. Interfaces* **2011**, *3*, 945–951.

[6] a) D. Fava, M. A. Winnik, E. Kumacheva, *Chem. Commun.* **2009**, 2571–2573; b) C. Wang, N. T. Flynn, R. Langer, *Adv. Mater.* **2004**, *16*, 1074–1079; c) R. R. Bhattacharjee, M. Chakraborty, T. K. Mandal, *J. Phys. Chem. B* **2006**, *110*, 6768–6775.

[7] a) H. Zhang, D. Wang, *Angew. Chem.* **2008**, *120*, 4048–4051; *Angew. Chem. Int. Ed.* **2008**, *47*, 3984–3987; b) M. Yang, G. Chen, Y. Zhao, G. Silber, Y. Wang, S. Xing, Y. Han, H. Chen, *Phys. Chem. Chem. Phys.* **2010**, *12*, 11850–11860; c) H. Zhang, K. H. Fung, J. Hartmann, C. T. Chan, D. Y. Wang, *J. Phys. Chem. C* **2008**, *112*, 16830–16839.

[8] X. Han, J. Goebl, Z. Lu, Y. Yin, *Langmuir* **2011**, *27*, 5282–5289.

[9] K. G. Hans-Jürgen Butt, Michael Kappl, *Physics and Chemistry of Interfaces*, Wiley-VCH, Weinheim, **2003**.
[10] P. Pramod, K. G. Thomas, *Adv. Mater.* **2008**, *20*, 4300 – 4305.
[11] C. Girard, E. Dujardin, M. Li, S. Mann, *Phys. Rev. Lett.* **2006**, *97*, 100801.
[12] a) M. Djabourov, A. H. Clark, D. W. Rowlands, S. B. Ross-Murphy, *Macromolecules* **1989**, *22*, 180 – 188; b) J. Narayanan, J.-Y. Xiong, X.-Y. Liu, *J. Phys. Conf. Ser.* **2006**, *28*, 83.
[13] D. L. Feke, N. D. Prabhu, J. A. Mann, J. A. Mann, *J. Phys. Chem.* **1984**, *88*, 5735 – 5739.
[14] B. V. Enustun, J. Turkevich, *J. Am. Chem. Soc.* **1963**, *85*, 3317.
[15] a) J. Richardi, *J. Chem. Phys.* **2009**, *130*, 044701 – 044709; b) M. Elimelech, J. Gregory, X. Jia, W. R. A, *Particle Deposition and Aggregation - Measurement, Modelling and Simulation*, Elsevier, **1998**.
[16] J. Liu, W. Y. Shih, M. Sarikaya, I. A. Aksay, *Phys. Rev. A* **1990**, *41*, 3206 – 3213.
[17] V. A. Parsegian, G. H. Weiss, *J. Colloid Interface Sci.* **1981**, *81*, 285 – 289.
[18] a) A. Revil, P. A. Pezard, P. W. J. Glover, *J. Geophys. Res.* **1999**, *104*, 20021 – 20031; b) R. Venditti, X. C. Xuan, D. Q. Li, *Microfluid. Nanofluid.* **2006**, *2*, 493 – 499; c) A. Revil, D. Hermitte, E. Spangenberg, J. J. Cocheme, *J. Geophys. Res.* **2002**, *107*; d) P. M. Reppert, F. D. Morgan, *J. Geophys. Res.* **2003**, *108*.
[19] J. A. Long, D. W. J. Osmond, B. Vincent, *J. Colloid Interface Sci.* **1973**, *42*, 545 – 553.
[20] J. Bentz, S. Nir, *Proc. Natl. Acad. Sci. USA* **1981**, *78*, 1634 – 1637.

